Surface Morphology of Syndiotactic Polypropylene Single Crystals Observed by Atomic Force Microscopy

Vladimir V. Tsukruk*

College of Engineering & Applied Sciences, Western Michigan University, Kalamazoo, Michigan 49008

Darrell H. Reneker*

Institute of Polymer Science, The University of Akron, Akron, Ohio 44325

Received June 21, 1994; Revised Manuscript Received October 28, 1994®

ABSTRACT: We have studied the surface morphology of single crystals of syndiotactic polypropylene (sPP) by atomic force microscopy (AFM). The thickness of a single crystal lath grown at 140 °C was determined by AFM to be 10.5 ± 1 nm. The surface roughness within flat, defect-free areas up to 1 μm across was in the range 0.3−1 nm. A feature of the sPP single crystals was straight cracks about 100 nm wide across the single crystal laths. Three to four cracks were observed on a single-crystal with the average distance between adjacent cracks of 5−10 μm. Smooth periodic undulations in thickness, or wrinkles, were observed. The periodicity of these undulations is about 400 nm and the number of periods can reach 10−30. On the molecular scale, we observed modulations of surface topography with periods of 1.5 and 1.1 nm that are close to the lengths of the *a* and *b* edges of the sPP unit cell determined from electron diffraction.

Introduction

Mechanical and physical properties of partially crystalline bulk polymers depend upon features of their spherulitic supramolecular organization built by "stacks" of lamellar crystals. The formation of specific spherulitic structures upon characteristics of a single lamella and lamellar growth toward definite supramolecular organization. The ideal models for polymer lamellar crystals are isolated single crystals grown from solution.[1,2] Controlled nucleation and growth of various crystals of polymeric result in the formation of ideal single crystals in basic shapes such as lozenge-shaped crystals for polyethylene and lath-like crystals for polypropylenes.[1−3] Stress-free growth of crystals from solution produces large single crystals with very smooth surfaces. Crystal surfaces formed by regularly folded macromolecular chains have roughness values in the range 0.3−0.6 nm, as measured by atomic force microscopy (AFM).[4] Fold domain boundaries and patches of one to two monomeric unit heights were observed for various polymer single crystals by transmission electron microscopy (TEM) and confirmed by recent AFM observations.[4] Periodic molecular features on AFM molecular images were attributed to regular arrays of chain folds.[4b] Friction force microscopy revealed significant differences in the frictional distribution of neighboring fold domains related to an abrupt change in orientation of chain folds.[4c]

Mechanical distortions and tensions that occur naturally during the formation of the crystalline phase affect crystal growth and the resulting morphology and properties of partially crystalline polymers. Applied mechanical stresses might distort and deform the ideal surface morphology of polymer single crystals and result in the distortion of the supramolecular organization of crystalline polymers. For example, fractures caused by *external* tensile stress were observed in lamellar structures of polymer single crystals.[5] On the other hand, it was demonstrated that the isothermal growth of polymer single crystals at different conditions can produce a variety of crystals with periodic modulations in thickness.[6] Besides, detailed TEM observations of Lovinger et al.[6] show the existence of *spontaneous* transverse fractures in isothermally-grown single crystals of syndiotactic polypropylenes (sPP) due to *internal* local stresses. These observations were associated with the highly anisotropic thermal contraction of the sPP crystal lattice during isothermal growth and following fast cooling of the crystals. The formation of similar periodic modulations of the surface of growing thin films in the presence of stress was analyzed by Grinfeld and Srolovitz[7−9] and was observed experimentally for some solids.[10,11] The authors demonstrated that in stressed growing solids, surface diffusion can lead to the relaxation of stress via formation of periodic surface perturbations with a characteristic wavelength. The question arises whether this kind of surface instability can be produced by crystal growth under thermally induced steady stresses and observed for crystalline lattices of polymers.

Thus, in fact, it was demonstrated that even stress-free growth of polymer crystals might result in fractures and deformations of ideal crystal habits. Obviously, these deviations may play a crucial role in the formation of highly hierarchical supramolecular organization in partially crystalline polymers and affect their mechanical properties. Therefore, very initial stages of polymer crystal growth which can be a subject of local mechanical tensions require detailed morphological investigations.

Single crystals of sPP provide a good model to examine the possible occurrence of surface disturbances caused by mechanical stresses. First, the morphology of these crystals is very suitable for detailed structural investigations. Within a definite temperature interval, crystals of sPP are grown with a lath-like habit, which provides an unambiguous identification of the arrangement of surface features with respect to the crystal lattice. Second, X-ray data show a high anisotropy of thermal expansion coefficients in the temperature range

* To whom correspondence should be sent.

® Abstract published in *Advance ACS Abstracts,* January 1, 1995.

0024-9297/95/2228-1370$09.00/0

from room temperature to 145 °C. The thermal expansion coefficient along the b-axis of the unit cell is about 1 order of magnitude higher than along the a-axis.[6] This leads to almost pure uniaxial stress in the crystal subjected to a change in temperature, with the stress along the b-axis about 1 order of magnitude greater than along the a-axis. Third, the mobility of the macromolecules is large enough to permit the surface to rearrange as the crystals cool. Diffusion of the macromolecules is relatively high because the glass transition temperature is around room temperature.[12]

Another intriguing circumstance is that for sPP different models of molecular packing were recently reported in the crystalline phase.[13-17] The different parameters and symmetries of the unit cells were derived from electron diffraction and X-ray scattering data. Two different orthorhombic modifications were observed for different preparation conditions. A model of molecular structures for the single crystals on the basis of electron diffraction data was proposed by Lovinger et al.[13,14] As was shown, the unit cell of isothermally grown single crystals of sPP has parameter $a = 1.45$ nm, $b = 1.12$ nm, and $c = 0.74$ nm. The macromolecules form a helix with its axis in the c direction. Right and left hand helices alternate in the $a \times b$ plane. The c-axis is normal to the lamellar surface, and the b-axis is along the longer axis of the lath single crystal.[6,13] A different unit cell was proposed for the crystals in sPP fibers.[15,16] Thus, the determination by independent experimental technique of the unit cell that occurs in these crystals provides an additional challenge.

Experimental Section

Single crystals of sPP were prepared by isothermal crystallization of ultrathin films by A. Lovinger, AT&T. The crystals have been grown at 130–145 °C (melting range is 150–170 °C) according to a procedure decribed earlier.[13,14] Single crystals were grown for periods ranging from 3 to 24 h, and then rapidly cooled to room temperature. Optical phase contrast microscopy, TEM, electron diffraction, and X-ray analysis were used to characterize single crystal shape, surface morphology, and local molecular packing in refs 6, 13, and 14. These data, along with X-ray results for the thermal expansion of the sPP lattice mentioned above, are used here for analysis of the AFM measurements.

An AFM technique was selected as a primary method to investigate surface morphology with great details.[18,19] AFM provides a way to observe the surface structure of polymer single crystals at the micron and molecular scales.[4,18] Unlike classic microscopic techniques, the AFM technique allows the acquisition 3D topographic data with a high vertical resolution (down to 0.05 nm) in selected areas with lateral sizes at the nanometric scale. The accurate and quantitative data about surface morphology can be provided in a wide range of magnifications and interpreted firmly by taking into account possible artifacts introduced by a finite size of the AFM tip.[4,18] A combination of electron microscopic and scattering techniques with the AFM observations can produce a pool of quantitative and unambiguous data about surface topography which surpasses current knowledge.

AFM images of the surfaces were obtained in air and in water with an atomic force microscope, the Nanoscope II (Digital Instruments, Inc.), using a pyramidal Si_3N_4 tip. Imaging was performed according to well established procedures for polymeric materials.[4] Different heads J, D, and A were used for scanning with applied forces of 10^{-8} N in air and 10^{-9} N in water. Cantilevers with a spring constant of 0.38 N/m and scan rates of 1–2 Hz were used for low and medium magnifications. For the highest magnifications, scan rates were 6–20 Hz. All AFM data are presented as obtained, except some molecular imaged which were filtered by a Fourier transformation (see below). Images of the surfaces of the polymer crystals are reproducible in repeated scans of the same area. Scanner A was calibrated using the mica standard. Gold coated optical gratings with 1 μm spacing and grids with 10 μm cell size were used for calibration of scanners D and J.

Results and Discussion

General Review of Surface Morphology. The surface morphology of sPP single crystals grown at different temperatures is described in detail in ref 6, 13, 14, and 17. All these observations were done and conclusions were made on the basis of TEM and confocal optical microscopy experiments. It was demonstrated that the variation of growth temperature yields a spectrum of morphologies ranging from lath-like habit to spherulitic supramolecular organization through multilamellar crystal growth and screw dislocations.

Before we discuss some novel observations of surface morphology obtained by the AFM technique we have to compare our results with well established morphological data for these crystals. An analysis of our data leads to a conclusion that all general features of sPP single crystal morphology observed by optical microscopy and TEM are confirmed by AFB observations in the same range of magnifications. Various morphological habits observed are shown in Figures 1 and 2. Axialites of sPP grown from an isolated nucleus are usually composed of three to six lath-like single crystals (Figure 1a,b). These laths are 20–50 μm long and 5–15 μm wide. The height of a single crystal of sPP is 10.5 ± 1 nm, which agrees fairly well with TEM estimates. Crystals with two or three superposed lamellae with regions 22 and 33 nm thick are occasionally observed (Figures 1c and 2a).

The surface roughness in the area of 100 nm × 100 nm is 0.3–0.8 nm, indicating that these surfaces are flat and smooth. The roughness in the areas of 2 μm × 2 μm is much higher and reaches 3 nm. These larger areas include variations of lamellar thickness from edge to center, accumulations of polymer materials along the edges of crystals, and tiny islands of undeveloped nuclei, as can be seen in Figures 1c,d and 2c, respectively. Multilamellar structures and irregular ridges that grew along the edges of the lath crystals held at crystallization temperature for prolonged times were observed (see Figure 1c,d).

Some other details of surface morphology are shown in Figure 2. Edges of two crystals, which may be part of the same growth spiral, are visible in Figure 2a. These crystals are both 10.5 ± 1 nm and have the same orientation. The profiles of their edges differ significantly (Figure 3). One edge has a sharp step profile of about 11 nm, while a 3–4 nm deep groove is observed near the other edge. The observed difference does not depend upon scanning direction and is reproducible after repeated scanning. We could speculate that this might reflect a different mechanism of growth and material supply along the a and b edges of the two crystals.

At micron scale, the surface of sPP crystals possesses a variety of interesting morphological details. For example, Figure 2b shows multiple sharp ridges aligned along the a direction on top of the single crystals. They are straight and as thin as 0.2 μm, with heights in the range 10–40 nm. These ridges are surrounded by tiny nanofibers with diameters of 3–5 nm. A large number of sharp ridges about 10 nm high were observed along the a edges of the single crystals as well (Figure 1d). As was discussed in ref 14, these features are dendritic nuclei formed probably from low molecular fractions of

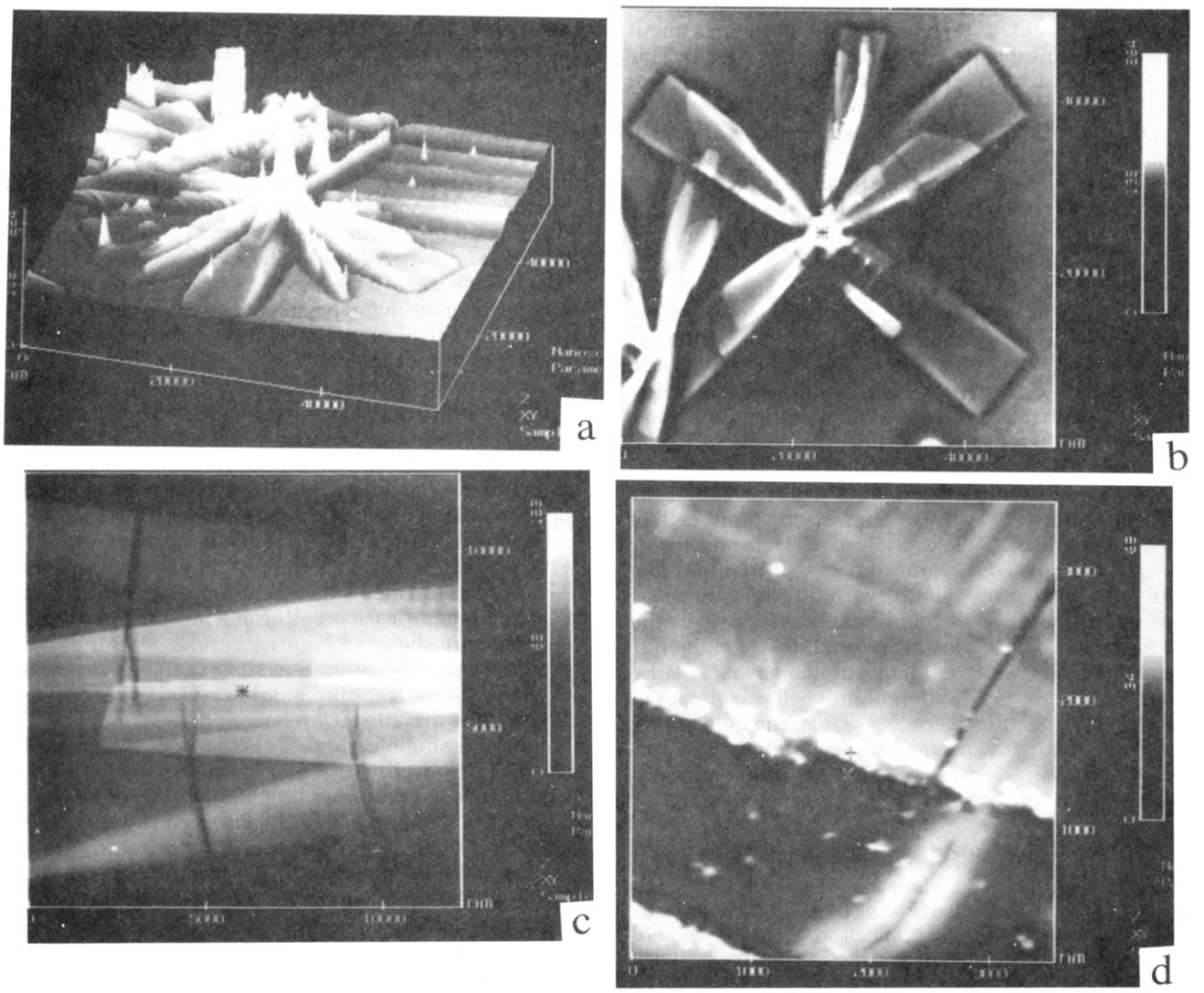

Figure 1. AFM images of the lath-like single crystals at low magnifications: (a) three-dimensional image of the single crystals grown from an isolated nucleus, scan size is 48 μm × 48 μm; (b) top view of the single crystals grown from an isolated nucleus, 45 μm × 45 μm; (c) fragment of the lath-like single crystal with multilamellar structures, surface undulations, and fractures, 12 μm × 12 μm; (c) the edge of the single crystal with accumulated ridges, surface undulations, fractures, and undeveloped nuclei, 3.5 μm × 3.5 μm.

the polymer. The tiny undeveloped centers of crystallization or nuclei of dendritic crystals were observed between two single crystals on a film surface and also on top of the single crystals (see Figure 1d). At higher magnification, in Figure 2c it can be seen that they have diameters in the range 100−200 nm and heights 6−10 nm. The surrounding 0.5−1 μm long fibrillar-like arms have diameters of 2−5 nm. These arms are undeveloped lath-like crystals that could form axialites similar to the one shown in Figure 1a.

The sPP single crystals are very stable under the substantial compressive and shear mechanical stresses produced by the AFM tip.[4] All areas can be scanned repeatedly without visible damage of the surface. All the observed features are stable and can be reproduced with consistent geometrical parameters for different mechanical loads, scanning rates, and orientation of scanning. To check the mechanical stability of a polymer surface, a "scratch" test can be used.[19] A high load of 200 nN on the AFM tip during scanning of a small area with a high scan rate leads to local deformation of the polymer crystal and the formation of holes of one or two lamellar thicknesses deep, as shown in Figure 2d. The holes are rectangular, with smooth edges, and indicate that the mechanical properties of the lamellar crystals are similar along the a and b directions. Obviously, no brittle fracture of the polymer surface occurs around the hole, and the hole is a result of plastic deformation.

Periodic patterns that include many periods of undulations and straight microcracks running across the total width of the single crystals are distinguished features of the crystal surface (see Figures 1c,d and 4a−c). As we mentioned above, this kind of surface perturbation was observed by Lovinger et al. and Cheng et al. in TEM studies of sPP single crystals.[6,17] Periodic surface undulations and microcracks run across the main axis of the lath-like crystals. The long dimension of each undulation is therefore transverse to the b-axis of the crystalline lattice (Figures 1c and 4a). The undulations are higher and more evident near the edges of the crystals. Three to four cracks are observed in 20−40 μm lengths of lath crystals, while 10−30 periodic undulations, running parallel to the microcracks, are observed in the same region.

The AFM technique provides quantitative information about actual profiles of observed surface features that are unavailable from TEM.[4,18] An example of the sinusoid-like profile of modulated surfaces is presented in Figure 5a. The periodicity λ and amplitude A of these

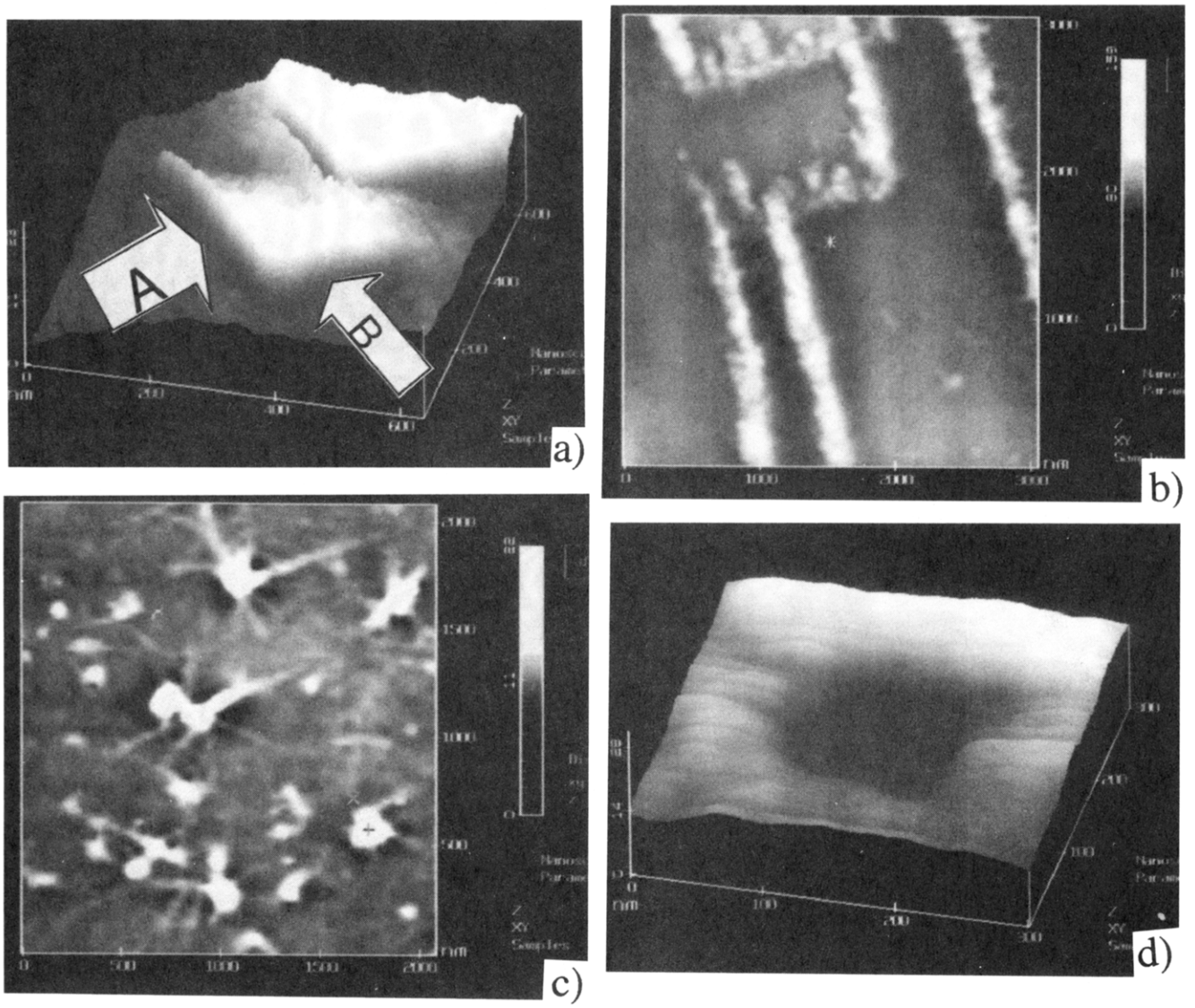

Figure 2. AFM images of the features of surface morphology at higher magnifications: (a) the corner of the double lamellar crystal, 620 nm × 620 nm (cross section profiles shown in Figure 3 were taken as shown by arrows); (b) ridges along the long axes of the single crystals on the surface of a single crystal, 3 μm × 3 μm; (c) undeveloped nuclei of single crystals, 2.1 μm × 2.1 μm; (d) artificially produced hole, 80 nm × 80 nm across, in the lamellar crystal, 300 nm × 300 nm.

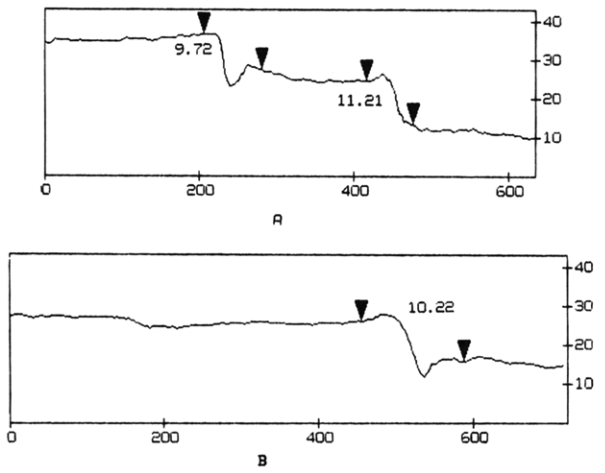

Figure 3. Profiles of the single crystal edges along the normal to the edges of the double crystal imaged in Figure 2a. Cross section places are shown in Figure 2a with arrows. Numbers between the markers indicate the vertical distance between the neighboring markers. All distances and scales are in nanometers.

undulations averaged over different single crystals are $\lambda = 400 \pm 120$ nm and $A = 6 \pm 3$ nm. The half-width of the microcracks is 90 ± 30 nm, as shown by the markers on the cross-section in Figure 5a. The crack depth corresponds to the thickness of the multilamellar crystal and is therefore about 10, 20, or 30 nm depending upon how many stacked lamellae are fractured. An analysis of the observed disturbances shows that many details of perturbed surface morphology are consistent with mechanism of surface instabilities driven by surface diffusion and can be satisfactory described by a theory proposed in refs 7–9. Detailed discussion of this phenomena will be published elsewhere.[30]

Occasionally, we observed some other surface features. For example, the cracks sometimes run along the top of the surface undulations or an irregular crack propagates along the long axis of the lath-like crystals (Figure 4c). High, periodic ridges are occasionally formed on top of the single crystals (Figure 4d). These ridges are separated by distances of 2–4 μm (see cross-section in Figure 5b) and are superposed on the surface undulations. The formation of these ridges can be attributed to material pushed away from the crystal during growth, but the actual mechanism of this phenomena is unclear now.

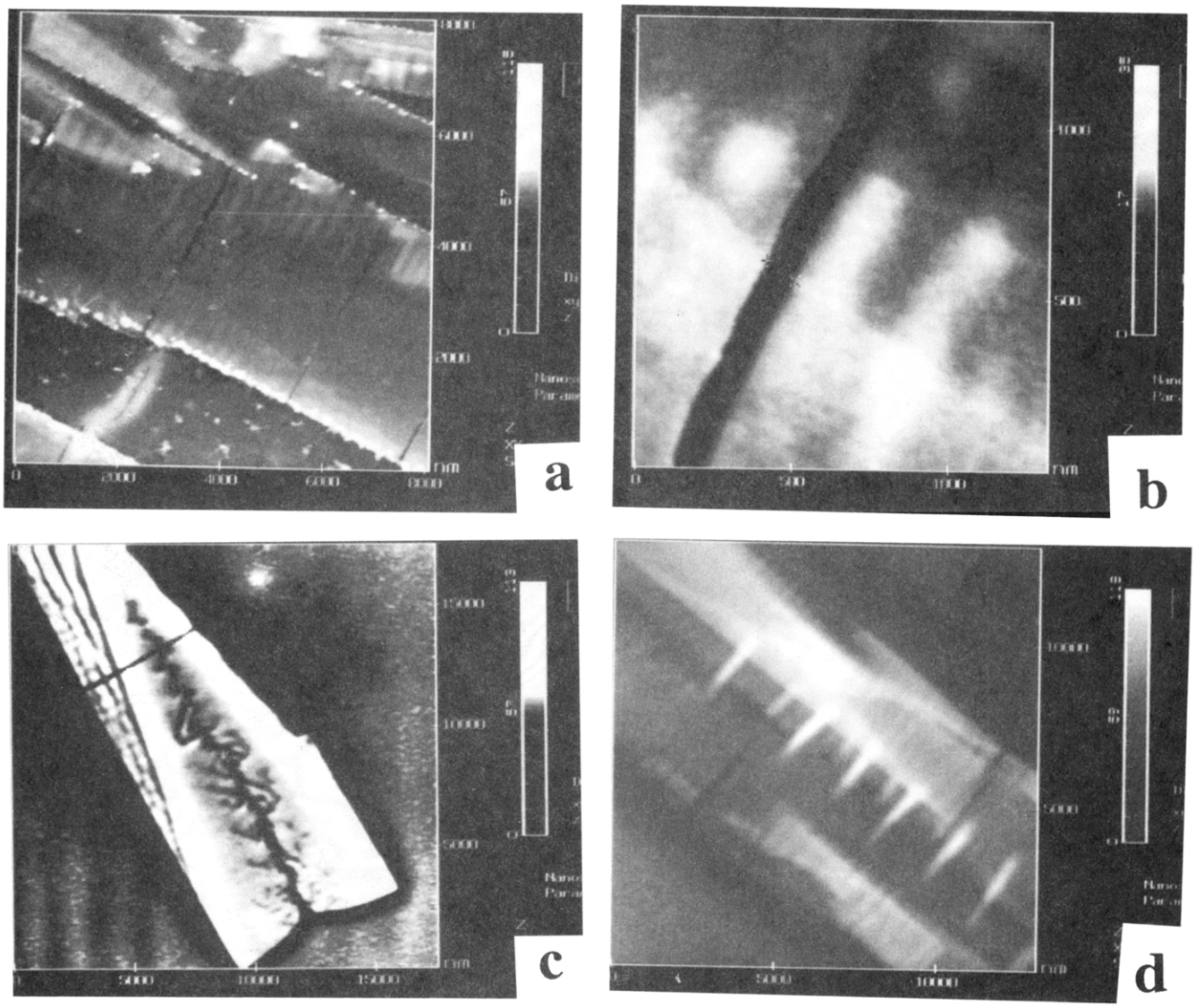

Figure 4. AFM images of crystal surface undulations and fractures: (a) the edges of the single crystals with transverse undulations and cracks, 8 μm × 8 μm; (b) the crack edges at higher magnification, 1.3 μm × 1.3 μm; (c) irregular crack along the *b*-axis, 17 μm × 17 μm; (d) area with long periodic ridges overlapping surface undulations, 13 μm × 13 μm.

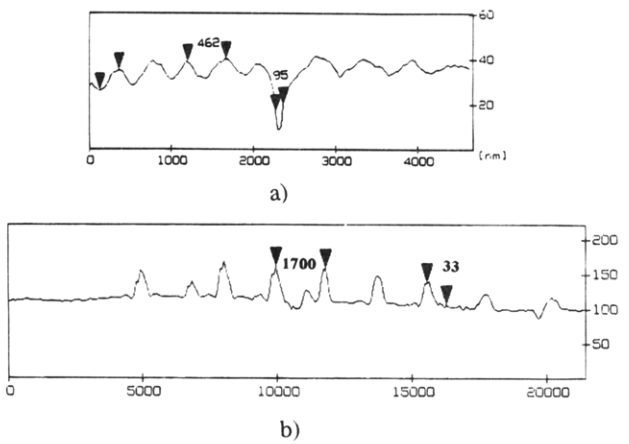

Figure 5. Cross sections of the single crystal surface along the long axes: (a) periodic undulations and fracture profile, 4.6 μm length; (b) large perturbations at the surface with a 1.7 μm long period, 22 μm length. The numbers are the horizontal distance between the neighboring markers for (a) and the left pair of the markers in (b); 33 nm is the vertical distance between the markers in (b). All distances and scales are in nanometers.

Molecular Ordering. Scanning in air did not produce stable molecular images of the single crystal surface. We had to switch to imaging in a fluid cell. Reduction of the tip forces in water (about 1 order of magnitude) made it possible to obtain reliable surface topography with nanometer scale features (Figure 6a,b). Molecular size features with similar periods were constantly observed at various parts of the single crystal surface. To avoid artificial features, all electronic filters were kept off during scanning at the nanometer scale. The proportional and integral grains were in the range of 4−6 (in the terms of Nanoscope II software). Scanning rates were 6−20 Hz. A typical molecular image without digital processing is presented in Figure 6b. Weak modulations with periods of about 1.5 nm running vertically and about 1.0 nm running horizontally in the image were observed.

The periods observed on these images were emphasized by the Fourier filtration procedure (Figure 6c). Only sharp Fourier components with periods in the range 0.2−2 nm were retained during the filtration procedure (see insert in Figure 6c). A fragment of the resulting enhanced image as shown in Figure 6c. On this image, a lattice structure with periods between bright molecular ridges of 1.5 nm in the horizontal direction and 1.1 nm along the vertical direction are clearly visible. Weaker ridges are located between these

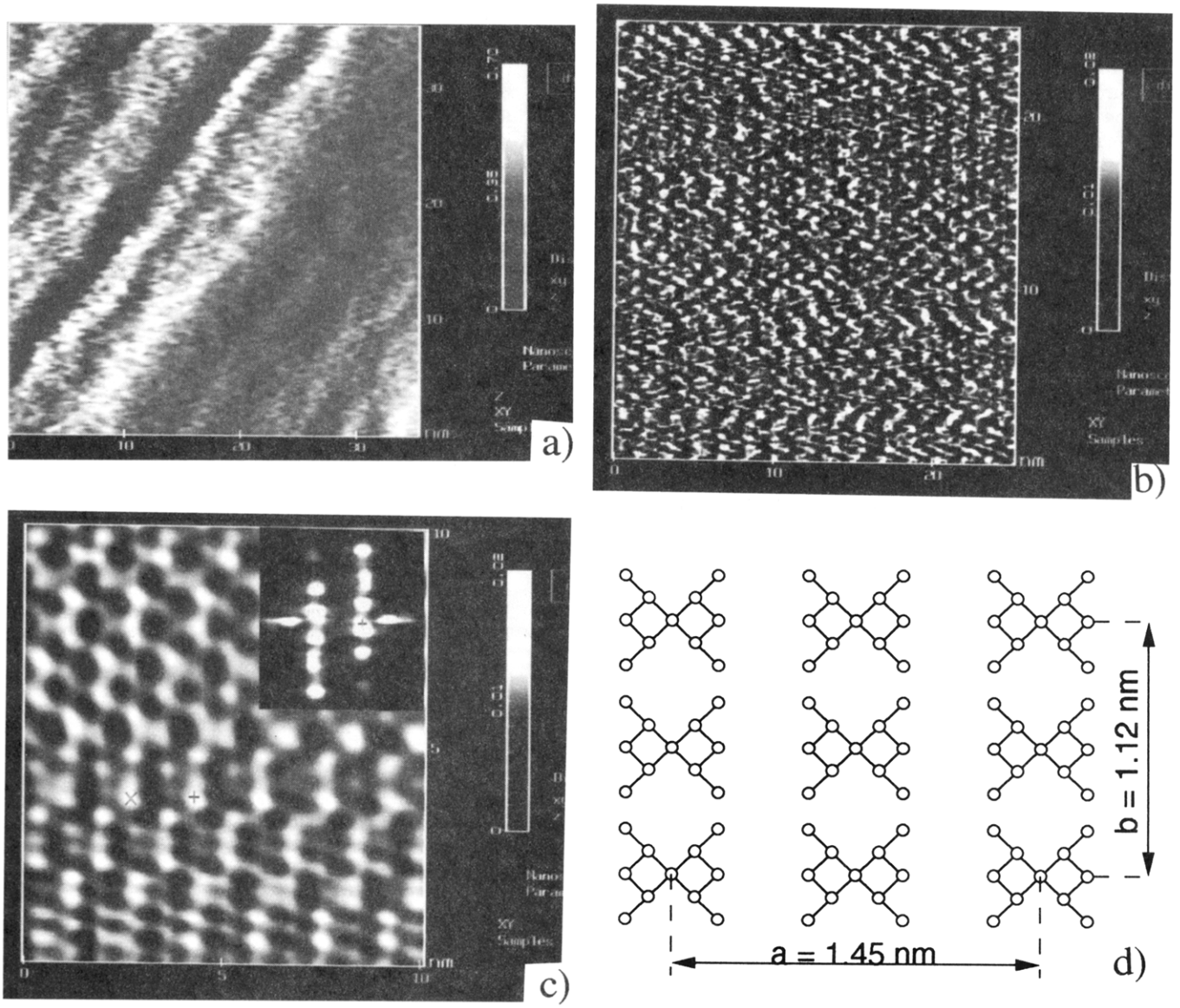

Figure 6. Molecular scale images of the single crystal surface: (a) typical surface topography at flat areas, 35 nm × 35 nm; (b) as-obtained molecular image, 24 nm × 24 nm; (c) a selected area of the image (b) with Fourier filtration, retaining only the most intense components, 10 nm × 10 nm (the insert is the 2D Fourier-transformation of image (b)); (d) $a \times b$ plane of the unit cell with the parameters and molecular arrangements proposed[13].

features, corresponding to a shorter period of 0.75 nm in the horizontal direction and 0.6 nm in the vertical direction on the image.

The next step is comparison of the observed arrangement of molecular ridges with parameters of the $a \times b$ lattice plane (Figure 6c). A horizontal periodicity of 1.5 ± 0.1 nm fits quite well to the length of the a edge of the unit cell (1.45 nm). A vertical periodicity of 1.1 ± 0.1 nm corresponds to the length of the b edge of the unit cell. The presence of additional molecular elements in the center and along the edges of the cell corresponds quite fairly to the molecular arrangement in the orthorhombic centered unit cell proposed by Lovinger et al.[13,17] Therefore, the geometric parameters of the observed molecular images are consistent with the unit cell proposed on the basis of electron diffraction data for the sPP single crystals.[13] Orientation of the molecular ridges along the b edge with deep minima between ridges along the a-axis can be associated with the folds running along the b-axis of the unit cell. This agrees with the conclusions made in ref 17 on the basis of TEM observations. The resolution of the molecular images does not allow a more detailed analysis of the molecular arrangement.

Conclusions

All general features of sPP single crystal morphology observed by optical microscopy and TEM are confirmed by AFM observations in the same range of magnifications. Axialites of sPP grown from an isolated nucleus are usually composed of three to six lath-like single crystals with total heights of 10.5 ± 1 nm. Crystals with 2 or 3 superposed lamellae with thicknesses of 22 and 33 nm are occasionally observed. The local surface roughness is 0.3−1 nm, indicating that the lamellar surfaces are flat and smooth. The most interesting features include: an increase of lamellar thickness from the center of the edge of unknown nature, accumulations of materials along the edges of the crystals in the form of dendritic nuclei, multilamellar structures that grew along the edges of the lath crystals, sharp ridges aligned along the a direction on top of single crystals, the undeveloped centers of crystallization observed on the substrate and on top of the single crystals, and periodic patterns that include many periods of undulations and straight microcracks running across the total width of the single crystals.

At the molecular scale, we observed surface topography in the form of molecular ridges on a regular lattice. The measured parameters of the unit cell are $a = 1.5 \pm 0.1$ nm and $b = 1.1 \pm 0.1$ nm. These periods are close to the lengths of the a edge and the b edge of the sPP unit cell determined from electron diffraction for similar sPP single crystals.[13] The orientation of the molecular ridges along the b-edge with deep minima between ridges along the a-axis can be associated with the folds running along the b-axis of the unit cell.

Acknowledgment. Funding for this research (V.V.T.) from the New Faculty Research Support Grant, Faculty Research and Creative Activities Support Grant, and Presidential Support for Research Activities, Western Michigan University, is gratefully acknowledged. The financial support of the Army Research Office is also gratefully acknowledged. The authors are very grateful to Dr. A. Lovinger (AT&T) for the samples of sPP single crystals supplied, encouraging interest and helpful discussions, and providing unpublished microscopy data and manuscripts.

References and Notes

(1) Geil, P. H. *Polymer Single Crystals*; Interscience: New York, 1963.
(2) Wunderlich, B. *Macromolecules Physics*; Academic Press: New York, 1976.
(3) Reneker, D. H.; Geil, P. H. *J. Appl. Phys.* **1960**, *31*, 1916.
(4) (a) Reneker, D. H.; Patil, R.; Kim, S.-J.; Tsukruk, V. V. In *Polymer Crystallization*; NATO Advanced Series; Doisere, M., Ed.; Kluwer Academic Press: London, 1993, *C405*, 357. (b) Patil, R.; Reneker, D. H. *Polymer* **1944**, *35*, 1909. (c) Nisman, R.; Smith, P.; Vancso, G. J. *Langmuir* **1994**, *10*, 1667.
(5) Reneker, D. H. *J. Polym. Sci. A* **1965**, *3*, 1069.
(6) Lovinger, A. J.; Davis, D.; Lotz, B. *APS Meeting*, Pittsburgh, March, 1994.
(7) Grinfeld, M. A. *Sov. Phys. Dokl.* **1986**, *31*, 831.
(8) Yang, W. H.; Srolovitz, D. J. *Phys. Rev. Lett.* **1993**, *71*, 1593.
(9) Srolovitz, D. J. *Acta Metall.* **1988**, *37*, 621.
(10) Torii, R. H.; Balibar, S. *Low Temp. Phys.* **1992**, *89*, 391.
(11) Berrehar, J.; Caroli, C.; Lapersonne-Meyer, C.; Schott, M. *Phys. Rev.* **1992**, *B46*, 13487.
(12) van Krevelen, D. W. *Properties of Polymers*; Elsevier: Amsterdam, 1980.
(13) Lovinger, A. J.; Lotz, B.; Davis, D. D.; Padden, F. J. *Macromolecules* **1993**, *26*, 3494. Rodriquez-Arnold, J.; Zhang, A.; Cheng, S.; Lovinger, A.; et al. *Polymer* **1994**, *35*, 1884.
(14) Lovinger, A. J.; Davis, D. D.; Lotz, B. *Macromolecules* **1991**, *24*, 552.
(15) Rosa, C. D.; Corradini, P. *Macromolecules* **1993**, *26*, 5711.
(16) Auriemma, F.; Rosa, C. D.; Corradini, P. *Macromolecules* **1993**, *26*, 5719.
(17) Lovinger, A. J.; Lotz, B.; Davis, D.; Schumacher, M. *Macromolecules*, to be published.
(18) Frommer, J. *Angew. Chem., Int. Ed. Engl.* **1992**, *31*, 1298.
(19) Tsukruk, V. V.; Reneker, D. H. *Polymer*, accepted.
(20) Tsukruk, V. V.; Reneker, D. H. *Phys. Rev. B*, **1995**, *51*, N5.

MA941152F